Comparison of Structural Concepts for Transport Aircraft with a Tail Cone Turbine

Brian H. Mason[*]

NASA Langley Research Center, Hampton, VA, 23681-2199

An evaluation of three structural concepts for an advanced aircraft design with a tail cone turbine is presented. Structural models were developed using an innovative rapid finite element modeling tool called Conceptual Design Shop (CDS). CDS is an attempt to fill a gap in current finite element modeling software to automatically connect wings and tails to the fuselage with sufficient support structure in airframe models. For comparison with actual aircraft structures, a model of a transport aircraft design developed using CDS is compared with published structural weight data for a Boeing 737-200. A method for computing aerodynamic stability parameters from an MSC/NASTRAN finite element analysis output deck is also discussed. Finally, the weight effects for using a tail cone turbine in an advanced transport aircraft design are evaluated by comparing three composite structural models, for which component thicknesses and cross-sections are sized by the Hypersizer software.

I. Introduction

A. Motivation and Background

NASA's Advanced Air Transport Technology (AATT) project is tasked with drastically reducing fuel consumption, noise, and emissions in the next generation of commercial aircraft. One promising technology that AATT is considering is the use of more advanced, efficient electrical aircraft components with high power densities. New turboelectric propulsion technologies are being devised that are powered by generators attached to existing hydrocarbon fuel-burning turbomachinery. Examples of these technologies include distributed fans and boundary layer ingestion (BLI), which increase the propulsion efficiency and reduce the vehicle wake. One BLI concept under consideration by NASA is the single-aisle turboelectric aircraft with an aft boundary layer propulsor (STARC-ABL).

STARC-ABL is a tube-and-wing concept with two underwing mounted turbofans. Each turbofan is attached to a generator that converts mechanical fan shaft power to electrical power. This additional electrical power is used to run a BLI tail cone turbine (TCT). The STARC-ABL concept was developed to determine if the turboelectric propulsion system is beneficial when simply added to an existing conventional transport configuration without completely redesigning the propulsion system. However, the aft section of the fuselage must be redesigned to incorporate the TCT; so, conceptual design studies are required. To date, most studies involving STARC-ABL are primarily focused on aerodynamic and propulsion system performance [1, 2], and structural weight is computed using historically-based weight estimation equations [3]. Historical structural weight data for traditional aircraft is unlikely to be accurate as advanced aircraft geometries evolve beyond traditional tube-and-wing design; so, a study of the effects of incorporating concepts such as the TCT on the aircraft structural weight is needed.

Finite element (FE) modeling and analysis are the preferred techniques for computational simulation of structural responses. Unfortunately, generation of a complete airframe FE model is typically a labor-intensive process. Most available software for automated FE modeling only work with individual aircraft components such as the wing and fuselage [4-6], and have difficulty with the complicated wing/body interfaces between airfoil surfaces and the fuselage. A tool, called the Conceptual Design Shop (CDS), has been recently developed and used to successfully generate FE models of the STARC-ABL design [7].

Detailed structural data such as skin thickness and wing stiffness are rarely available from airframe manufacturers; however, structural weight data for major airframe systems of some aircraft are publicly available, and can be used for evaluation of structural models. In this paper, a FE model of a Boeing 737-200 is generated by CDS and compared against published structural weight data for that aircraft. The structural components of the 737 model are sized by structural optimization to satisfy buckling and strength constraints while subject to critical maneuver loads. After the Boeing 737 model (created with CDS) is developed, the metallic STARC-ABL models previously created using CDS [7] are sized using the composite materials used in other STARC-ABL studies [8].

---

[*]Research Aerospace Engineer, Structural Mechanics and Concepts Branch, Senior Member AIAA

B. Purpose and Contents

The purpose of this paper is to evaluate CDS as a tool for conceptual design of an airframe. Weight is a common metric used to evaluate conceptual structural designs; because, structural design information for existing aircraft is often proprietary. To evaluate CDS, the sized structural weight of a model developed using CDS was compared with historical data for a commercial transport aircraft. A Boeing 737-200 was selected for comparison due to its use in evaluation of another NASA tool called HCDStruct [4]. Additionally, CDS was used to study the weight effects of using a TCT on an advanced transport aircraft design. For this TCT study, two different aft fuselage concepts with a TCT were compared against a baseline concept without a TCT. The results of this study will be used by other NASA researchers working on STARC-ABL studies.

This paper is organized as follows. In Section II, the geometry and load conditions for the Boeing 737-200 and STARC-ABL models are discussed. In Section III, the analysis and results of the Boeing 737-200 comparison are presented. Results discussed in this section include structural weight, wing deflection, and aerodynamic stability and control parameters. A comparison of three STARC-ABL concepts sized with composite materials is described in Section IV. Future work for the CDS tool is described in Section V. Section VI contains a summary of the comparisons of the conceptual designs created with the CDS tool.

II. Model Geometry and Loads

In this section, the airframe FE models are described. Initially, as a check of the accuracy of the models generated by the CDS modelling tool, a model representing a Boeing 737-200 is discussed. Next, three models with different tail section concepts are discussed for a STARC-ABL aircraft design.

A. Conventional Aircraft Model

The CDS software uses planform geometry variables to define the wing and tail geometry of the airframe model. Planform variables used to generate the FE model of the Boeing 737-200 in CDS are presented in Table 1. Internal layout information in Table 1 is derived from standard aircraft design principles [9]. The geometry of the fuselage is input to CDS as an array of ring frame axial locations and cross-sectional points to define the shape of the ring frame. Fuselage parameters are currently input into the software using a text file. A fully meshed FE model of the 737 design is presented in Fig. 1. As illustrated in Fig. 1, the internal structure of the fuselage is coincident with the wing box structure of the wing and tail. The FE model consists of 11,958 nodes, 12,788 isoparametric membrane-bending shell elements, 465 beam elements, and 93 mass elements (representing fuel, landing gear, passengers, payload, and engine masses). The beam elements are used as spar and rib caps and in the floor, but not in the fuselage skin due to the additional programming required to split the fuselage panels at the stiffener locations (a current limitation of the software).

Table 1. Input parameters for 737-200 transport concept.

| Parameter	Wing	Horizontal Tail	Vertical Tail
Surface Area (sq. in.)	1,511,131	31,718	28,188
Aspect Ratio	7.940	3.491	1.491
Spanwise Break (%)	34.284	N/A	N/A
Taper Ratio at Break (%)	0.494	N/A	N/A
Taper Ratio at Tip (%)	0.222	0.459	0.375
Dihedral Angle at Root (deg)	1.856	7.000	0.000
Dihedral Angle at Tip (deg)	5.464	N/A	N/A
Sweep at Root Quarter-Chord (deg)	36.988	25.435	28.713
Sweep at Break Quarter-Chord (deg)	26.107	N/A	N/A
Forward Spar Location (% Chord)	25.000	24.383	30.000
Aft Spar Location (% Chord)	75.000	65.000	65.000
Thickness Ratio (% Chord)	0.120	0.120	0.120
X Location of Leading Edge Root (in.)	385.410	1052.921	950.000
Z Location of Leading Edge Root (in.)	-24.932	37.500	61.500
Number of Inboard Bays	11	5	5
Number of Outboard Bays	20	N/A	N/A
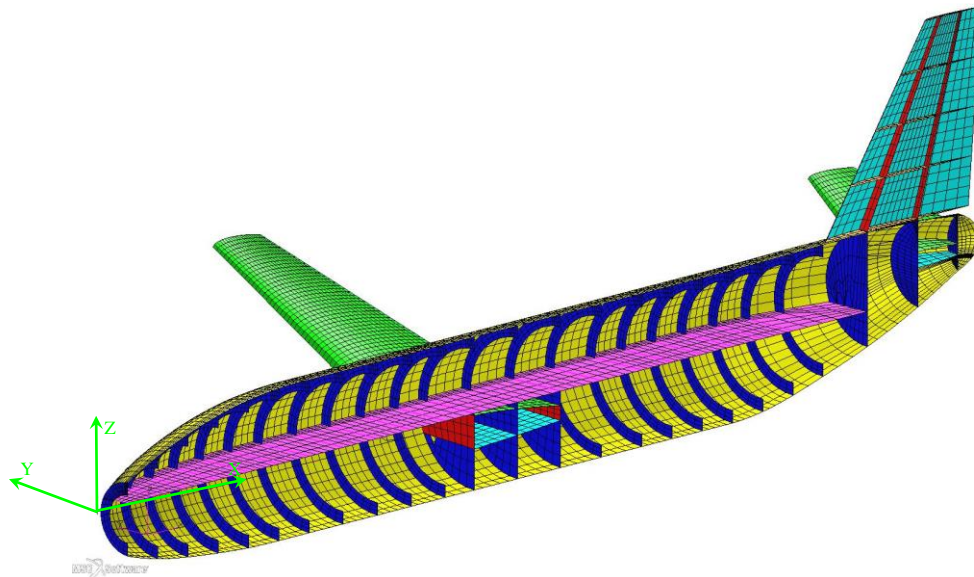
Figure 1. FE model of generic subsonic transport design (half-symmetry).

The analysis deck for the FE model is an MSC/NASTRAN[†] aeroelastic analysis deck [10]. In this MSC/NASTRAN deck, the wing planform, horizontal tail, and elevator surfaces are represented with aerodynamic doublet-lattice panels (CAERO1 and AELIST cards) to compute the aerodynamic forces. Nodes on the upper covers of the airfoil surfaces are automatically identified by CDS (grouped into SET1 cards) and associated with the aerodynamic panels using SPLINE4 cards. Cards to define the trim loading conditions (TRIM, AEROS, and PAERO1) and the airfoil downwash angles (DMI cards) are also generated. Downwash angles are computed at each spanwise and chordwise location as the slope of the mean camber line of the airfoil and the incidence angle of the wing. Three typical trim conditions [11] are considered in the aeroelastic analysis deck: 2.5-g positive limit maneuvering load, -1.0-g negative limit maneuvering load, and 1.0-g steady-state cruise flight. The cruise flight condition occurs at peak altitude for the aircraft (37,000 ft); therefore fuselage pressurization is included for this load case. All flight conditions are at a speed of 0.5 Mach and dynamic pressure of 1.760 psi.

B. Tail Cone Turbine Models

For the STARC-ABL design, three models with different aft fuselage sections were generated in CDS based on the concepts presented in Refs. 1 and 2. The first model (concept A) for the STARC-ABL design is presented in Fig. 2. The FE model consists of 18,313 nodes, 19,098 shell elements, 750 bar elements, and 86 mass elements. This concept is a baseline transport aircraft with a standard aft section without the TCT (as shown in Fig. 3). The other two concepts include the TCT. In the aft fuselage section of the second model (concept B, as shown in Fig. 4), a TCT is attached to the aft end of the fuselage from concept A using the two struts shown in red. For the third model (concept C, as shown in Fig. 5), the aft fuselage is narrowed to 60% of the diameter of concept B in order to increase the airflow to the TCT. The analysis decks for these models are MSC/NASTRAN aeroelastic analysis decks with the same load conditions as used in the Boeing 737-200 model.

[†] The use of trademarks or names of manufacturers in this report is for accurate reporting and does not constitute an official endorsement, either expressed or implied, of such products or manufacturers by the National Aeronautics and Space Administration.
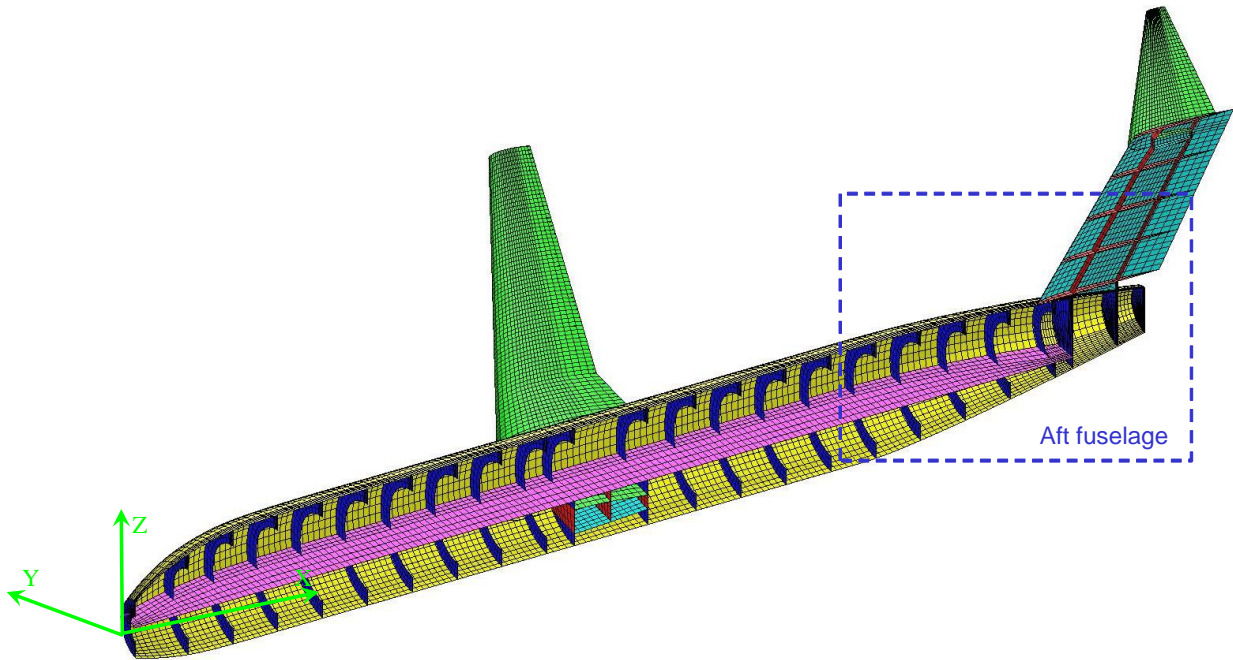
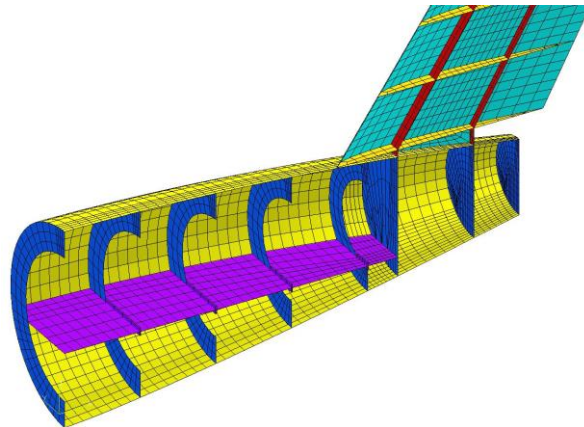**Figure 2.** FE model of STARC-ABL concept A (half-symmetry).

Figure 3. STARC-ABL concept A – baseline fuselage without TCT.
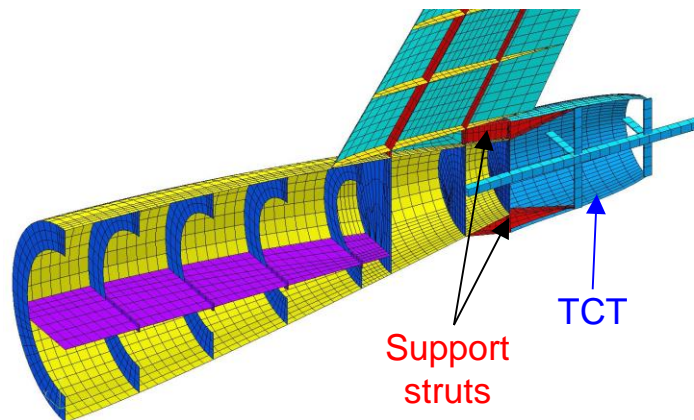

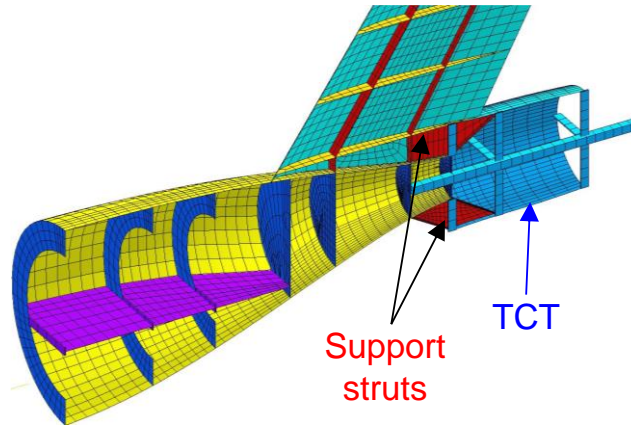**Figure 4.** STARC-ABL concept B – baseline fuselage with TCT.

Figure 5. STARC-ABL concept C – narrowed aft fuselage with TCT.

Planform variables used to generate the STARC-ABL designs for concepts A and B are presented in Table 2. In concept C, the location of the leading edge root for the horizontal and vertical tail is different from concepts A and B (the T-tail assembly was moved forward 48 in.).

Table 2. Input parameters for STARC-ABL transport concept.

Parameter	Wing	Horizontal Tail	Vertical Tail
Surface Area (sq. in.)	187,360	32,709	32,058
Aspect Ratio	9.974	6.084	1.400
Spanwise Break (%)	37.436	N/A	N/A
Taper Ratio at Break (%)	0.487	N/A	N/A
Taper Ratio at Tip (%)	0.198	0.202	0.800
Dihedral Angle at Root (deg)	6.000	6.000	0.000
Dihedral Angle at Tip (deg)	6.000	N/A	N/A
Sweep at Root Quarter-Chord (deg)	29.130	30.140	33.200
Sweep at Break Quarter-Chord (deg)	29.130	N/A	N/A
Forward Spar Location (% Chord)	25.000	23.800	30.000
Aft Spar Location (% Chord)	66.670	65.370	66.750
Thickness Ratio (% Chord)	0.120	0.120	0.120
X Location of Leading Edge Root (in.)	535.500	1383.372 (A & B) 1335.372 (C)	1236.706 (A & B) 1188.706 (C)
Z Location of Leading Edge Root (in.)	-36.000	251.555 (A & B) 259.055 (C)	57.000 (A & B) 64.500 (C)
Number of Inboard Bays	8	5	5
Number of Outboard Bays	19	N/A	N/A

III. Evaluation of Analytical Modeling Method for Boeing 737 Design

For the generic transport design, evaluation of the MSC/NASTRAN aeroelastic model is accomplished by comparison with as-built weight data for a Boeing 737-200 aircraft [12, 13]. Because details such as skin thicknesses and stiffener dimensions are not available, structural details for the FE model are obtained from a structural sizing to meet strength, buckling, and crippling constraints. Structural sizing of the FE model was performed using the Hypersizer software [14] with a 1.5 factor of safety applied to the aeroelastic loads. In Hypersizer, structural sizing is performed by defining minimum and maximum ranges for the sizing variables in each component. Then, each component is sized by finding the minimum weight component that satisfies structural constraints. All stiffener elements are sized as rectangular cross sections of aluminium 7075. The floor sections were sized as sandwich panels with aluminium 2024 face sheets and Hexcel 3.1 pcf core. All other shell elements were sized as unstiffened aluminium 2024 panels. The sized panel thicknesses are illustrated in Fig. 6. In Fig. 6, the wing thickness tapers from the root to the tip, and support structures (spars and bulkheads) are thickest at the wing/body interfaces.
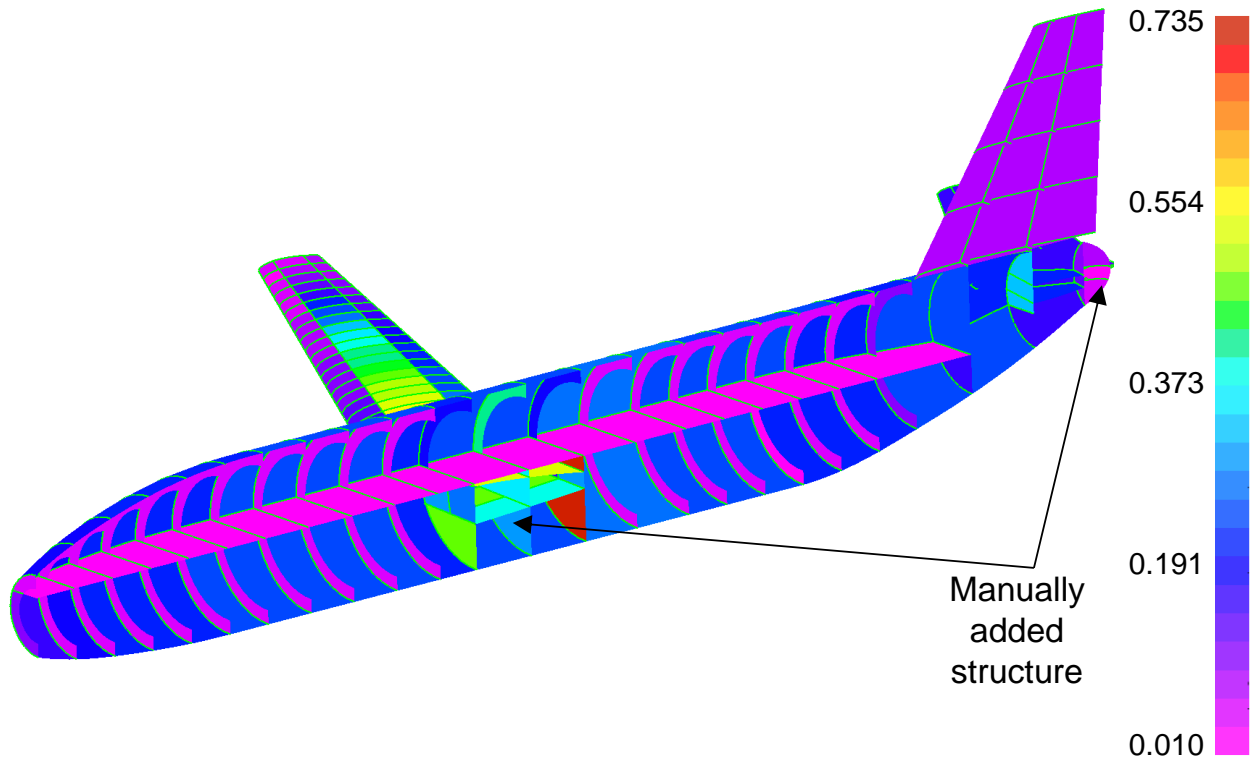
Figure 6. Sized panel thicknesses (in.) for the Boeing 737 model.

The NASTRAN analysis deck was generated by the CDS tool in under one minute on a desktop PC. Although CDS automatically generates the internal structure of an airframe; occasionally the load paths in airframe structures require manual addition of additional bulkheads or other internal structure. With the Boeing 737 model, a dome at the aft end of the fuselage and an additional bulkhead in the wing box in the fuselage were manually added to the CDS model to reduce local stresses. Additional changes were considered but not implemented. For example, because CDS did not generate stiffeners for the fuselage panels, Hypersizer makes the fuselage panels thicker than the ring frames. It is possible to define stiffener sizing variables for the panels in Hypersizer, but this was not done for this paper. The author had originally intended to compare the Boeing model in this paper with the model from another tool which also used unstiffened panels [11], but that did not occur due to project time constraints.

Note that the FE model is not an exact replica of the actual aircraft, but is expected to be a reasonable, conceptual-level approximation. The actual aircraft uses more efficient stiffened panels and includes access holes in the ribs and spars, which are not modelled for simplicity. Several large-mass non-structural items (fuel, passengers, payload, and controls systems) are represented by point masses, but fastener weights are not included. In spite of these differences, the structural model is in good agreement with the as-built weight (within 3% for the total structure) as shown in Table 3.

Table 3. Weight comparisons for the Boeing 737 model.

Component	Percent of As-built Structural Weight
Wing Structure	97.3%
Tail Structure	100.6%
Fuselage Structure	96.6%
Total Structure	**97.3%**

Additional aerodynamic stability and control data may be computed from the MSC/NASTRAN aeroelastic output deck (f06 file). One important stability parameter is the tail-on neutral point (NP), the axial location where the pitching moment of the aircraft is zero. The NP value is not part of the standard output of MSC/NASTRAN, but the NP can be easily computed from the MSC/NASTRAN output data by performing two analyses with different aerodynamic reference coordinate frames for rigid body motion (as defined in the AEROS card) and interpolating to

6

find the point that gives a pitching moment of zero. The pitching moment is labelled CMY in the reference coefficient section of the output deck. For example, with two coordinate systems with defined origins at x=0 and x=100 and corresponding pitching moment values of CMY_0 and CMY_{100}, respectively, the NP location (x_{NP}) can be computed using Equation 1. The axial center of gravity (x_{CG}), mean aerodynamic chord length (MAC), and NP can be used to compute the static margin (SM) using Equation 2 [9]. A positive value of SM means that the aircraft is longitudinally stable. For the Boeing 737-200 FE model, the static margin is stable at 16.6% as given in Table 4, which is expected for an in-service commercial aircraft. Similarly, from Table 4, angles of attack and elevator angles for trimming the aircraft are small (below 5%), which seem appropriate for a transport.

$$x_{NP} \; = \; 100 \left(\frac{CMY_0}{CMY_0 - CMY_{100}} \right) \qquad (1)$$

$$SM \; = \; \frac{x_{NP} - x_{CG}}{MAC} \qquad (2)$$

Table 4. Aerodynamic parameters for trim.

Component	Cruise	Climb	Dive
x_{CG} (from nose) (in.)		550.9	
Tail-On Neutral Point (in.)		578.5	
Static Margin (%)		16.6%	
Angle of Attack (deg)	0.62	4.32	-4.15
Elevator Deflection (deg)	-0.56	-4.60	3.79

IV. Comparisons of Alternative Tail Designs for STARC-ABL

For the STARC-ABL design, three concepts with different aft fuselage sections were generated in CDS. The aft fuselage section is considered to begin at longitudinal station 1040 in. and continue to the end of the 1400 in. long fuselage. Forward of the 1040 in. station, the geometry of all three FE models is identical. These three concepts were analyzed using the MSC/NASTRAN aeroelasticity analysis software. Three flight conditions were considered: 1.0-g cruise at 37,000 ft altitude with a fuselage pressure load, 2.5-g climb maneuver at 10,000 ft altitude, and -1.0-g dive maneuver at 10,000 ft altitude. Structural sizing was performed for each concept using the Hypersizer software [14] subjected to strength, buckling, and crippling constraints. For the structural sizing, a composite material system (AS4 carbon fiber [15]) is used. For each concept, at least three sizing iterations between Hypersizer and MSC/NASTRAN (to update the element-level forces) were performed, and convergence of the sizing process was defined as the point at which the weight change from one cycle to the next was less than 50 lb. (0.16% of the total structural weight). Although finite element model generation was automated in CDS, setting up the Hypersizer sizing study was a manual process. An Excel-based tool was used to extract the sizing results from Hypersizer. The sized panel thicknesses for STARC-ABL Concept C are illustrated in Fig. 7. Panel thicknesses for Concepts A and B were similar to C. As with the Boeing 737-200 model, the fuselage panels are unstiffened and are oversized. The thickest panels are at the wing/body interface and in the tail section. Of particular note is that the bulkhead at the aft tail spar location is very thick (1.77 in.) in order to support the weight of the TCT. The addition of additional bulkheads and spars in the tail would likely reduce the thickness of this bulkhead, but the weight of the added structure would offset the weight saved in this bulkhead, so the change was not implemented in this study. All three concepts exhibited this thick bulkhead, so the comparisons of the concepts with each other is still considered valid.
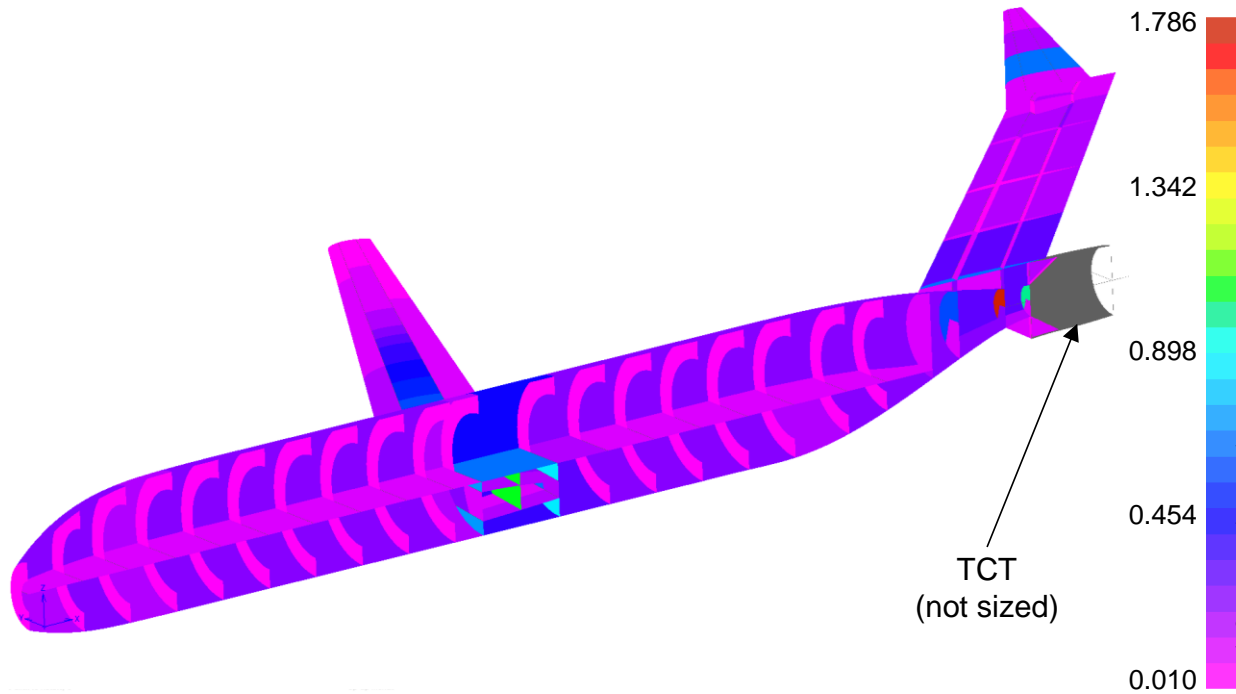
Figure 7. Sized panel thicknesses (in.) for the STARC-ABL Concept C model.

The forward fuselage weight is consistent among the three concepts, as presented in Table 5. In Table 5, the weights shown in red lettering were computed from the FE models, and the weights shown with a yellow background are fixed weights from Ref. 1 and 2. The aft fuselage of Concept C has a 25% smaller wetted area (345 sq ft) than Concepts A and B (460 sq ft) which is consistent with the 25% lower weight. The empennage weights of Concepts B and C include structural support for the TCT. The empennage of Concept B is 60% heavier than Concept A because of the lower static margin (given in Table 6) representing lower longitudinal stability and a corresponding increase in the horizontal tail loads. In Concept C, the forward shift of the horizontal tail reduces the length of the moment arm for trimming the aircraft, increasing the horizontal tail loads. While the increased horizontal tail loads in Concept C cause a significant increase in the empennage weight, this weight increase is offset by a decrease in the wing weight over Concepts A and B due to the decreased wing loading. Although Concept C has a lower structural weight than the baseline Concept A, this weight reduction is not enough to significantly reduce the 4,437 lb weight penalty of the TCT in Concepts B and C. Due to time constraints, an integrated systems analysis was not performed; so, the effects of the structural sizing on the fuel and engine weights are beyond the scope of this paper.

Table 5. Weight comparisons for three STARC-ABL concepts.

Component	Concept A	Concept B	Concept C
Wing (lb)	10,708	10,692	10,092
Forward Fuselage (lb)	15,231	15,231	15,263
Aft Fuselage (lb)	4,065	4,161	3,035
Empennage (lb)	1,252	2,005	2,117
Fuel (lb)	24,330	24,330	24,330
Wing Landing Gear (lb)	3,279	3,279	3,279
Passenger + Cockpit + Controls (lb)	56,845	56,845	56,845
Cockpit + Nose Landing Gear (lb)	3,618	3,618	3,618
TCT (lb)	**0**	**4,437**	**4,437**
3 Engines (lb)	8,855	8,855	8,855
GTOW (lb)	**128,183**	**133,453**	**131,872**
Delta Weight – Structural (lb)		833	-748
Delta Weight – GTOW (lb)		5,270	3,689

As with the Boeing 737 model, stability and control parameters were computed for the STARC-ABL concepts and are presented in Table 6. From Table 6, angles of attack and elevator angles for trimming the aircraft are small (below 7%) for all three concepts, which are typical for a transport aircraft. Concept B is the least stable design because of its heavier aft fuselage, but all concepts are stable (because of positive static margin values).

Table 6. Aerodynamic parameters for trim.

Component	Concept A	Concept B	Concept C
x_{CG} (from nose) (in.)	691.5	722.5	689.9
Tail-On Neutral Point (in.)	749.0	749.0	751.6
Static Margin (Cruise, %)	34.7	16.0	37.3
Angle of Attack (Cruise, deg)	-0.37	-0.38	-0.88
Angle of Attack (Climb, deg)	2.46	2.43	1.69
Angle of Attack (Dive, deg)	-3.67	-3.65	-3.65
Elevator Deflection (Cruise, deg)	1.98	4.28	4.20
Elevator Deflection (Climb, deg)	0.36	5.73	6.74
Elevator Deflection (Dive, deg)	1.95	0.01	-0.26

As an additional check on the size of the empennage control surfaces, the tail volume coefficients for the horizontal and vertical tails are computed for all three concepts. Torenbeek [16] suggests horizontal and vertical tail volume coefficients for transport aircraft of 1.01 and 0.074, respectively. As shown in Table 7, the vertical tail volume coefficient is above the recommended value of 0.074 for all concepts. The horizontal tail volume coefficient is between 12% and 18% lower than the recommended value of 1.01. The low horizontal tail volume coefficient indicates that increasing the area of the elevator control surface (which is currently 35% of the horizontal tail area) may improve the design and decrease the horizontal tail weight.

Table 7. Control surface parameters.

Component	Concept A	Concept B	Concept C
S, Wing Area (sq in.)		187,360	
Sh, Horizontal Tail Area (sq in.)		35,637	
Sv, Vertical Tail Area (sq in.)		32,058	
C, Mean Aerodynamic Chord of Wing (in.)		165.4	
B, Wing Span (in.)		1,367.0	
x_{CG} (from nose) (in.)	691.5	722.5	689.9
Xh, X location of Horizontal Tail Mean Aerodynamic Chord (in.)	1,460.9	1,460.9	1,412.9
Xv, X location of Vertical Tail Mean Aerodynamic Chord (in.)	1,345.5	1,345.5	1,367.0
Vh, Horizontal Tail Volume Coefficient	0.885	0.849	0.831
Vv, Vertical Tail Volume Coefficient	0.082	0.078	0.076

V. Limitations and Future Developments for CDS

Currently, the CDS software is limited to generating complete FE models of low-wing aircraft with T-tails, twin-tails, and conventional tails. However, CDS can be used to generate the components for different concepts, but the functions to generate these components and their interface surfaces are under development (including high-wing concepts and an improved fuselage frame definition procedure). Also, a Graphical User-interface (GUI) would be an improvement over the text file input approached currently used in CDS.

The current CDS system only creates half-symmetry models for static stress and static aeroelasticity analysis. These models can be modified to include flutter analysis. Also, the designs presented in this paper do not include lateral loads (which would require a full model, not a symmetry model), and do not include multi-disciplinary analysis to update the fuel loads and flight conditions based on changes to the structural weight. In this paper, the need for additional bulkheads in the wing and T-tail sections of the airframe were noted, and these structural components will need to be added to the automated design and modelling process in future versions of the CDS tool. Also, the CDS tool could be modified to either divide the fuselage sections at circumferential stiffener locations or assign the fuselage panels stiffened panel properties similar to the section properties used in the Hypersizer software.

VI. Summary

A study of the weight effects of using a TCT on an advanced transport aircraft design has been conducted within the AATT project. Many airframe conceptual design studies use historically-based weight estimation methods, but a more advanced method is used in this paper due to the unconventional geometry required to support a TCT. An innovative software for generation of complete FE models of airframe structures, called CDS, is used in the study in this paper. These airframe FE models are structurally sized to meet strength and buckling constraints and generate more accurate structural weights than values generated by historical estimation methods. As a check of the CDS models, the structural weight predicted by the FE model for a Boeing 737-200 is shown to compare well (within 3%) with the as-built structural weight.

CDS was used to evaluate three STARC-ABL concepts to evaluate the weight penalty for adding a TCT to the aft fuselage. Concept A was a baseline concept without a TCT. Concept B had the same geometry as Concept A, but added a TCT. In Concept C, the aft fuselage was narrowed for improved airflow to the TCT. Adding the TCT required an additional 833 lb of structure over the baseline concept to support the TCT. The structural weight of Concept C is 748 lb less than the baseline, but this is not enough to overcome the 4437 lb weight penalty of adding the TCT. Also, the horizontal tail volume coefficient is 12% to 18% too low; so improvements to the horizontal tail would increase its effectiveness and could possibly reduce the structural weight. Significant improvements in aerodynamic efficiency and fuel consumption with TCT would be necessary to significantly reduce the weight penalty and make the STARC-ABL a viable concept.

VII. References

[1]Kenway, G., X, "Aerodynamic Shape Optimization of the STARC-ABL Concept for Minimum Inlet Distortion," AIAA Paper 2018-1912, 59th AIAA/ASCE/AHS/ASC SDM Conference, Kissimmee, FL, January 2018.

[2]Welstead, J. R. and Felder, J. L., "Conceptual Design of a Single-Aisle Turboelectric Commercial Transport with Fuselage Boundary Layer Ingestion," AIAA Paper 2016-1027, 54th AIAA Aerospace Sciences Meeting, San Diego, CA, January 2016.

[3]McCullers, L., Aircraft Configuration Optimization Including Optimized Flight Profiles," NASA CP-2327, NASA, 1984.

[4]Gern, F., "Update on HCDstruct - A Tool for Hybrid Wing Body Conceptual Design and Structural Optimization," AIAA Paper 2015-2544, January 2015.

[5]Laughlin, T., Corman, J., and Mavris, D., "A Parametric and Physics-Based Approach to Structural Weight Estimation of the Hybrid Wing Body Aircraft," AIAA Paper 2013-1082, January 2013.

[6]Mukhopadhyay, V., Hsu, S., Mason, B. H., Sleight, D. W., Jones, W. T., Chu, J., Hicks, M. D., Spangler, J. L., Kamhawi, H., and Dahl, J. L., "Adaptive Modeling, Engineering Analysis and Design of Advanced Aerospace Vehicles," AIAA Paper 2006-2182, 47th AIAA/ASME/ASCE/AHS/ASC SDM Conference, Newport, Rhode Island, May 1-4, 2006.

[7]Mason, B. H. and Quinlan, J. R., "Conceptual Design Shop: A Tool for Rapid Airframe Structural Modeling," AIAA Paper 2018-2001, 59th AIAA/ASCE/AHS/ASC SDM Conference, Kissimmee, FL, January 2018.

[8]Welstead, J., Felder, J., Guynn, M., Haller, W., Tong, M., Jones, S., Ordaz, I., Quinlan, J., and Mason, B., "Overview of the NASA STARC-ABL (Rev. B) Advanced Concept," Presentation at One Boeing NASA Electric Aircraft Workshop, Washington, D.C., March 2017.

[9]Niu, M., Airframe Structural Design, Conmilit Press Ltd., 1988.

[10]MSC Software: NASTRAN Analysis Quick Reference Manual, MSC Software, Santa Ana, CA 92707.

[11]Quinlan, J. R. and Gern, F. H., "Aeroelastic Optimization of Generalized Tube and Wing Aircraft Concepts using HCDstruct Version 2.0," AIAA Paper 2017-0202, AIAA SciTech 2017 Conference, Dallas, TX, January 9-13 2017.

[12]Brady, C., The Boeing 737 Technical Guide, Tech Pilot Services Ltd., 2018.

[13]Boeing Commercial Airplanes, "Boeing 737: Airplane Characteristics for Airport Planning," Tech. Rep., The Boeing Company, 2013.

[14]*HyperSizer User's Manual, Book 1: Tutorial and Applications*, Collier Research & Development Corp., Hampton, VA, September 1998.

[15]Lovejoy, A. E. and Poplawski, S., "Preliminary Design and Analysis of an In-plane PRSEUS Joint", AIAA Paper 2013-1737, 54th AIAA/ASME/ASCE/AHS/ASC Structures, Structural Dynamics, and Materials Conference, Boston, MA, April 2013.

[16]Torenbeek, E., *Synthesis of Subsonic Airplane Design*, Delft University Press, Delft, The Netherlands, 1982.